Electronic Supplementary Information (ESI)

Photopatterning of fluorescent host-guest carriers through pore activation of metal-organic framework single crystals

I. Stassen,[a,b] I. Boldog,[a] C. Steuwe,[a] D. De Vos,[a] M. Roeffaers,[a] S. Furukawa[b] and R. Ameloot*[a]

[a] *Centre for Surface Chemistry and Catalysis, KU Leuven - University of Leuven, Celestijnenlaan 200F, Leuven 3001, Belgium. E-mail: rob.ameloot@kuleuven.be*
[b] *Institute for Integrated Cell-Material Sciences (WPI-iCeMS), Kyoto University, Yoshida, Sakyo-ku, Kyoto 606-8501, Japan.*

Contents

ESI-1. Experimental procedures

Purity of chemicals. All chemicals were used as commercially obtained, unless specified otherwise. All manipulations were carried out in air; using dimmed light conditions and darkened glassware during manipulation of the photosensitive compounds.

Synthesis of linkers. Experimental details for the synthesis of 2-((2-nitrobenzyl)oxy)terephthalic acid (**L_1**), 2,5-di((2-nitrobenzyl)oxy)terephthalic acid (**L_2**) and 2,2'-bis-((2-nitrobenzyl)oxy)-biphenyl-4,4'-dicarboxylic acid (**L_3**) are described in section **ESI-3**.

Synthesis of IRMOF crystals. The procedures for synthesis of **IRMOF-1**, **IRMOF-1-L_1/L_2** and **IRMOF-10-L_3** was based on a general protocol for fabrication of large crystals of multivariate IRMOFs reported by Yaghi *et al*.[1] Glass crimp cap reactor vials (10 mL) were thoroughly rinsed with purified water to remove dust particles and dried under air flow at 60 °C. 20 mL precursor solutions were prepared according to the following table:

	$Zn(NO_3)_2.6H_2O$	**Linker**	**Solvent**
IRMOF-1	4.53 mmol (1.347 g)	benzene-1,4-dicarboxylic acid: 1.53 mmol (0.251 g)	diethylformamide
IRMOF-1-L_1/L_2	1.20 mmol (0.356 g)	**L_1**: 0.16 mmol (0.051 g) **L_2**: 0.24 mmol (0.112 g)	diethylformamide
IRMOF-10-L_3	0.36 mmol (0.106 g)	**L_3**: 0.13 mmol (0.072 g)	dimethylformamide

The precursor solutions were first passed through 0.6 µm PTFE membrane filters and then each divided over three to four reactor vials. The vials were sealed and placed in an aluminum heating block inside an isothermal oven at 82 °C for 48 h. The resulting crystals were washed three times with copious amounts of dehydrated DMF and stored in the same solvent at room temperature.

Heteroepitaxial core-shell assemblies were fabricated using an elegant strategy reported by Matzger *et al*.[2] In this method, **IRMOF-1** and **IRMOF-1-L_1/L_2** were crystallized in parallel using the procedures described above. After 24 h, the respective precursor/reaction solutions were quickly exchanged, *i.e.* the **IRMOF-1** seed crystals were immersed in the solution for growth of **IRMOF-1-L_1/L_2**. In the next growth phase, the synthesis vials were gently agitated once every few hours while placed in an isothermal oven at 82°C, in order to make sure that shell growth could occur at all faces of the cubic crystals (avoiding permanent contact of a certain face with the glass container). After 24 h of heteroepitaxial crystal growth at 82°C, core-shell assemblies consisting of an **IRMOF-1** core and **IRMOF-1-L_1/L_2** shell were obtained (**IRMOF-1-L_1/L_2@IRMOF-1**). Importantly, in a typical synthesis batch, only a few core-shell crystals at most were found that showed a fully intact shell capable at excluding organic dyes from entering the core.

Characterization. Bulk photochemical reactions on 10 mg of the linker dissolved in 650 µl dimethyl sulfoxide-d_6) were conducted at room temperature by placing screw-capped transparent glass vials in a home-built photoreactor equipped with a set of Hitachi FL8BLBL lamps (UV-A; 300-400 nm). Samples were taken at different time points and analyzed by NMR. The crystal structure of the samples was verified using a batch of ca. 10 solvated crystals and a Rigaku Smartlab X-ray diffractometer equipped with a Cu Kα source; and using a hand-picked monocrystal and a Rigaku AFC10 diffractometer with Rigaku Saturn CCD system equipped with a Mo Kα source. Digital optical microscopy was used to assess the shape and size of the synthesized crystals using a Keyence VHX-5000 microscope. To verify the degree of deprotection of the

incorporated linkers in **IRMOF-1-L_1/L_2** and **IRMOF-10-L_3**, ca. 15 crystals of each synthesis batch were digested in in a mixture of 650 µl dimethyl sulfoxide-d_6 and 10 µl 35 % deuterium chloride in D_2O. The resulting solutions were analyzed by NMR. Excitation and emission spectra of 100 µM solutions of the different dyes in dimethylformamide were obtained using a Hitachi F-7000 fluorescence spectrophotometer (240 nm min^{-1} scan rate at 400 V PMT).

Spatial selective photochemical activation and confocal microscopy. A number of MOF crystals were placed on a microscopy slip fixed in a homebuilt epifluorescence liquid microscopy cell. Next, 1 mL of dehydrated dimethylformamide was added to submerge the crystals, as well as two to four dehydrated zeolite molecular sieve beads (5Å, Sigma Aldrich) in order to keep the solvent dry. The cell was placed on the stage of a confocal laser scanning microscope (CLSM, Olympus FV1000) or two-photon laser scanning microscope (Zeiss LSM 780 equipped with Mai Tai Deep See Femtosecond Ti:Sa laser). For spatial selective photochemical activation, the 405 nm continuous wave laser, or 800 nm pulsed laser, were scanned in a designated area of the crystal using the microscope software, typically using the following settings:

- 405 nm laser — 5 % power (≈ 2.5 mW power; measured at focal point of UPLSAPO20x N.A. 0.75 objective lens), 0.20 µm step size between each irradiated pixel, 10 µs dwell at each pixel, 200 repeated scans, 15 to 30 µm focus depth,
- 800 nm laser — 2 % power (≈ 50 mW average power; measured at focal point of LD LCI Plan-Apochromat 25x N.A. 0.8 objective lens), 0.17 µm step size between each irradiated pixel, 0.6 µs dwell at each pixel, 200 repeated scans, 20 to 50 µm focus depth.

The dye solutions were added immediately after the photochemical activation procedure. The crystals were subsequently imaged by CLSM using the same microscopy cell and emission/excitation and gain settings that were independently adjusted for each utilized dye. Data plotting was conducted using the Olympus FV10-ASW4.2 viewer, Zeiss ZEN (blue edition, 2.3 lite) and the freely available software package ImageJ Fiji 1.51j.[3]

ESI-2. Supporting experiments and figures

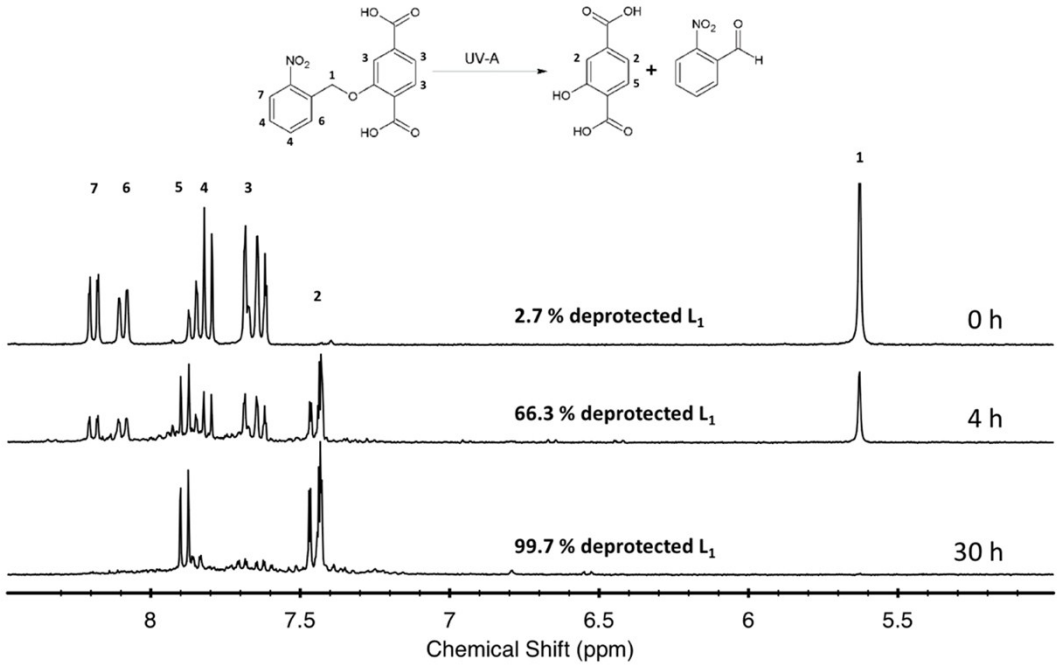

Figure S1. ^{1}H NMR spectra of **L_1** linker before UV-A exposure (0 hours), after 4 hours of UV-A exposure, and after 30 hours of UV-A exposure. The degree of deprotection (%) was calculated using the ratio of peak group 2 (7.45 ppm; m; 2H; H-Ar) and peak 1 (5.63 ppm; s; 2H; CH_2).

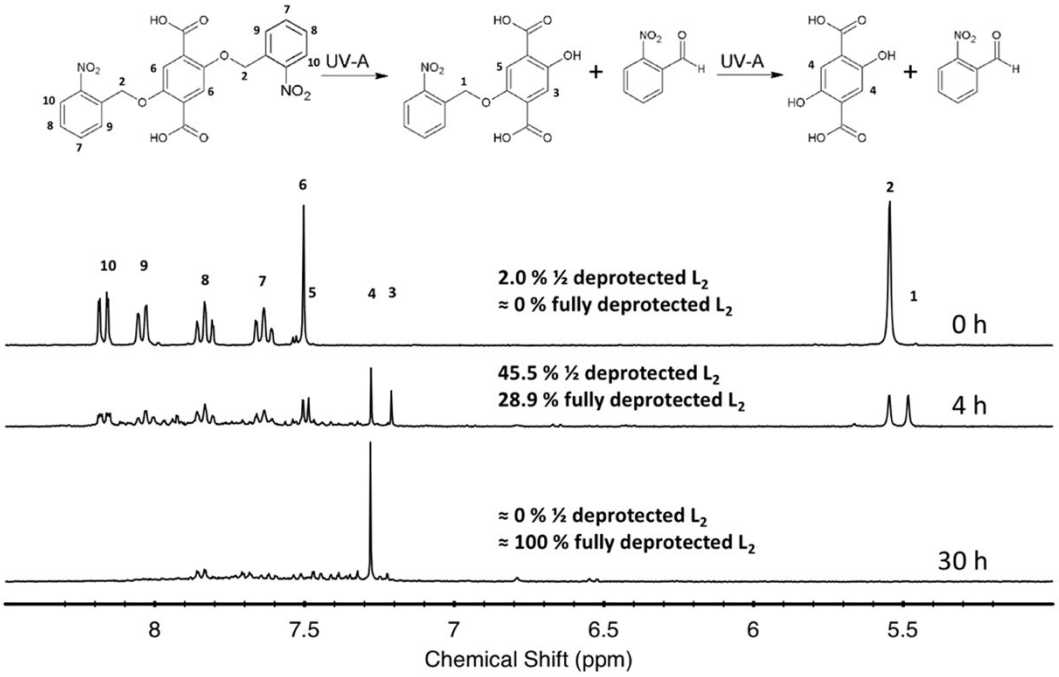

Figure S2. ^{1}H NMR spectra of **L_2** linker before UV-A exposure (0 hours), after 4 hours of UV-A exposure, and after 30 hours of UV-A exposure. The degree of deprotection (%), either with one photolabile group

cleaved (½ deprotected) or both groups cleaved (fully deprotected), was calculated using the ratios of peak 1 (5.45 ppm; s; 2H; CH_2), peak 2 (5.55 ppm; s; 4H; CH_2) and peak 4 (7.30 ppm; s; 2H; H-Ar).

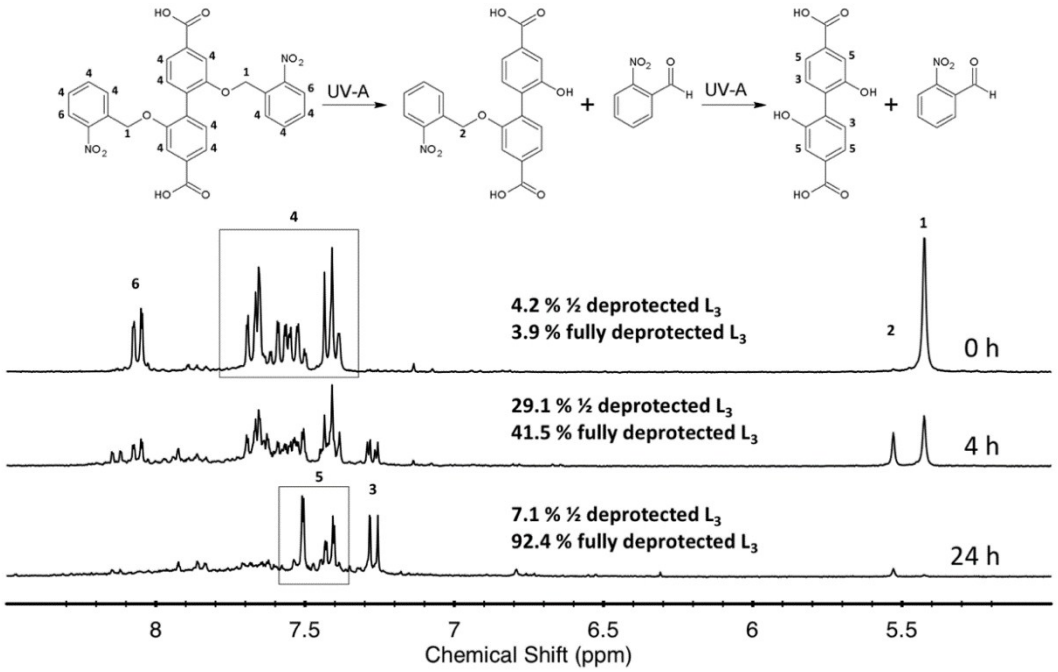

Figure S3. ^{1}H NMR spectra of **L_3** linker before UV-A exposure (0 hours), after 4 hours of UV-A exposure, and after 24 hours of UV-A exposure. The degree of deprotection, either with one photolabile group cleaved (½ deprotected) or both groups cleaved (fully deprotected), was calculated using the ratios of peak 1 (5.45 ppm; s; 4H; CH_2), peak 2 (5.55 ppm; s; 2H; CH_2) and peak 3 (7.28 ppm; d; J= 7.9; 2H; H-Ar).

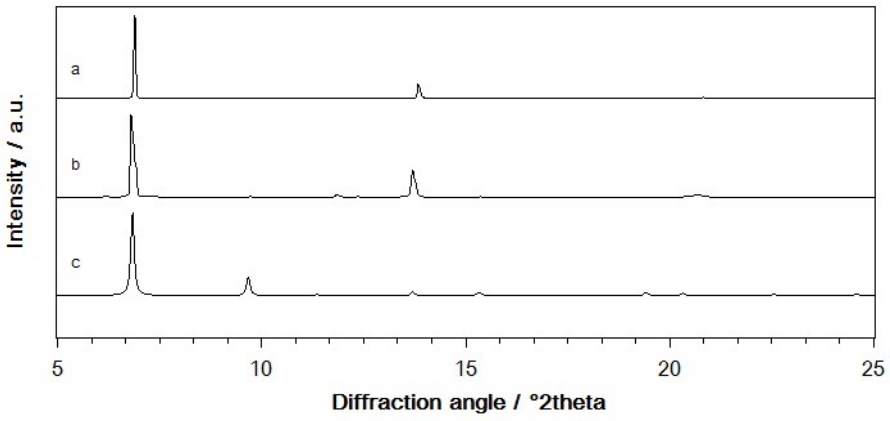

Figure S4. PXD pattern of a) **IRMOF-1-L_1/L_2** b) **IRMOF-1** c) **IRMOF-1** CSD Refcode EDUSIF.

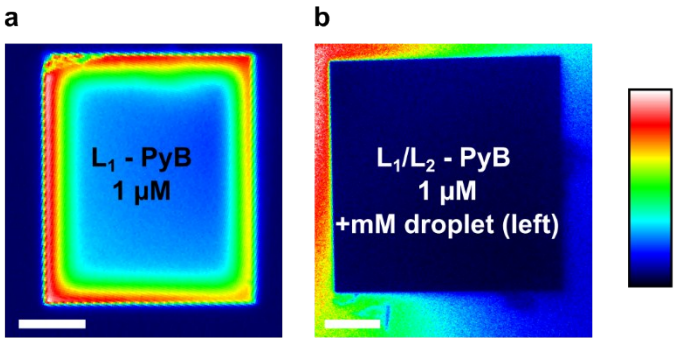

Figure S5. CLSM images of Pyronin B at 25 µm height inside two **IRMOF-1-L$_1$** and **IRMOF-1-L$_1$/L$_2$** crystals after 2 h soaking in 1 µM solution. a. Slow penetration of Pyronin B into the crystal of **IRMOF-1-L$_1$**. b. No visible penetration into the crystal for **IRMOF-1-L$_1$/L$_2$**. A droplet of 1 mM Pyronin B was added seconds before imaging to demonstrate the comparable detection range of both experiments. The relative intensity scale is shown in the bottom of the panel (0-4095 a.u.). Scale bars 50 µm.

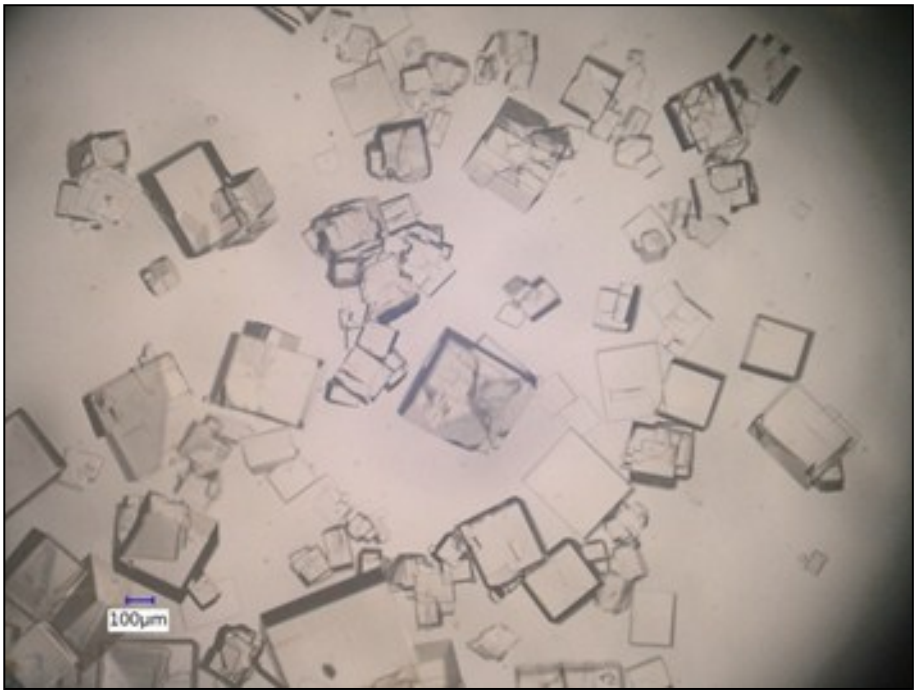

Figure S6. Light microscopy image of **IRMOF-1** single crystals; colorless. Scale bar: 100 µm.

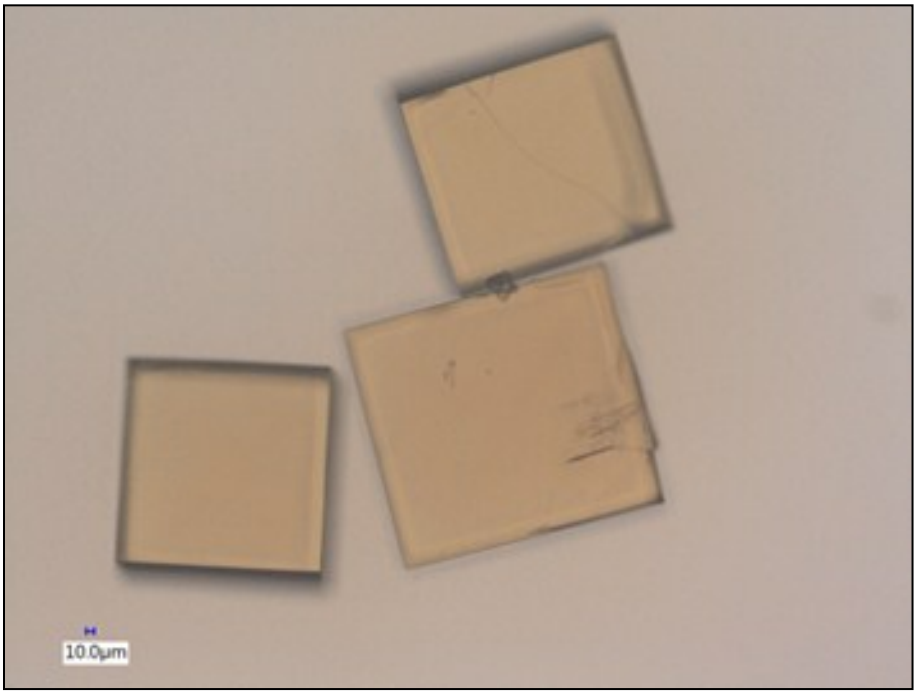

Figure S7. Light microscopy image of **IRMOF-1-L_1/L_2** single crystals; faint yellow. Scale bar: 10 µm.

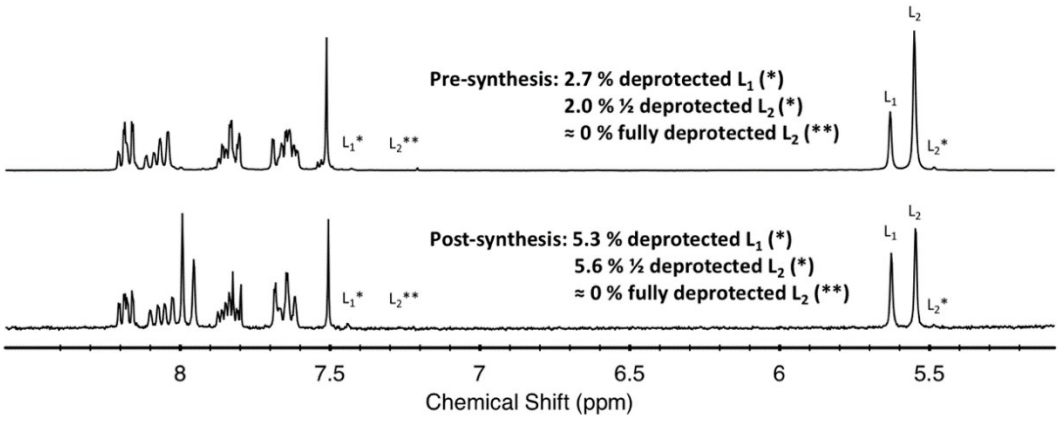

Figure S8. ^{1}H NMR spectra of a mixture of linker **L_1** and linker **L_2** (≈ 40:60 ratio) in DMSO-d_6 (pre-synthesis), and **IRMOF-1-L_1/L_2** dissolved in a D_2O/DMSO-d_6 solution (post-synthesis). The percentage of **L_1** and **L_2** in **IRMOF-1-L_1/L_2** was calculated using the peaks at 5.55 ppm (s; 4H; CH_2) and 5.63 ppm (s; 2H; CH_2). The percentage of post-synthesis deprotection was analyzed using the peaks described in Figure S1-2.

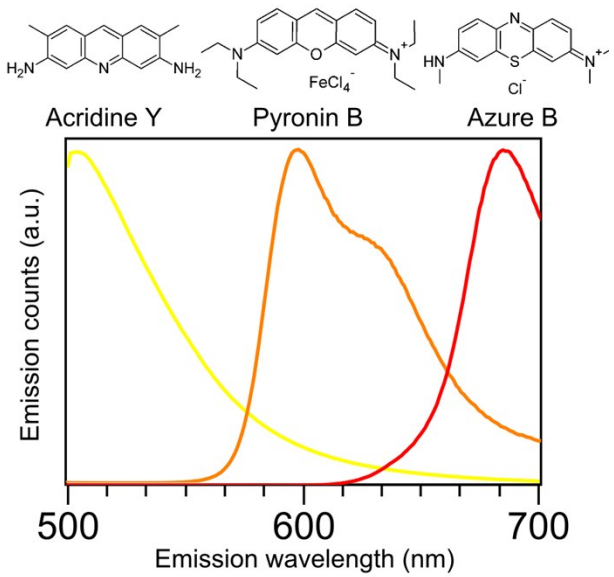

Figure S9. Emission spectra of Acridine Y (excitation at 488 nm), Pyronin B (excitation at 559 nm) and Azure B (excitation at 635 nm); chemical structures are shown at the top for each dye.

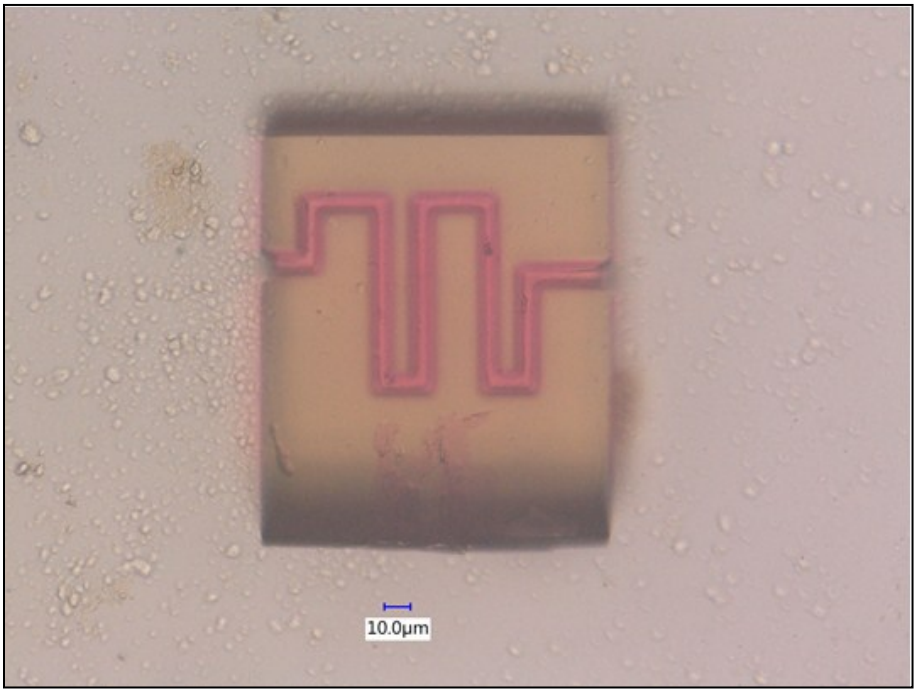

Figure S10. Bright-field optical microscopy image showing the crystal shown in Figure 2c of the article after transferring to and soaking in fresh DMF for several hours.

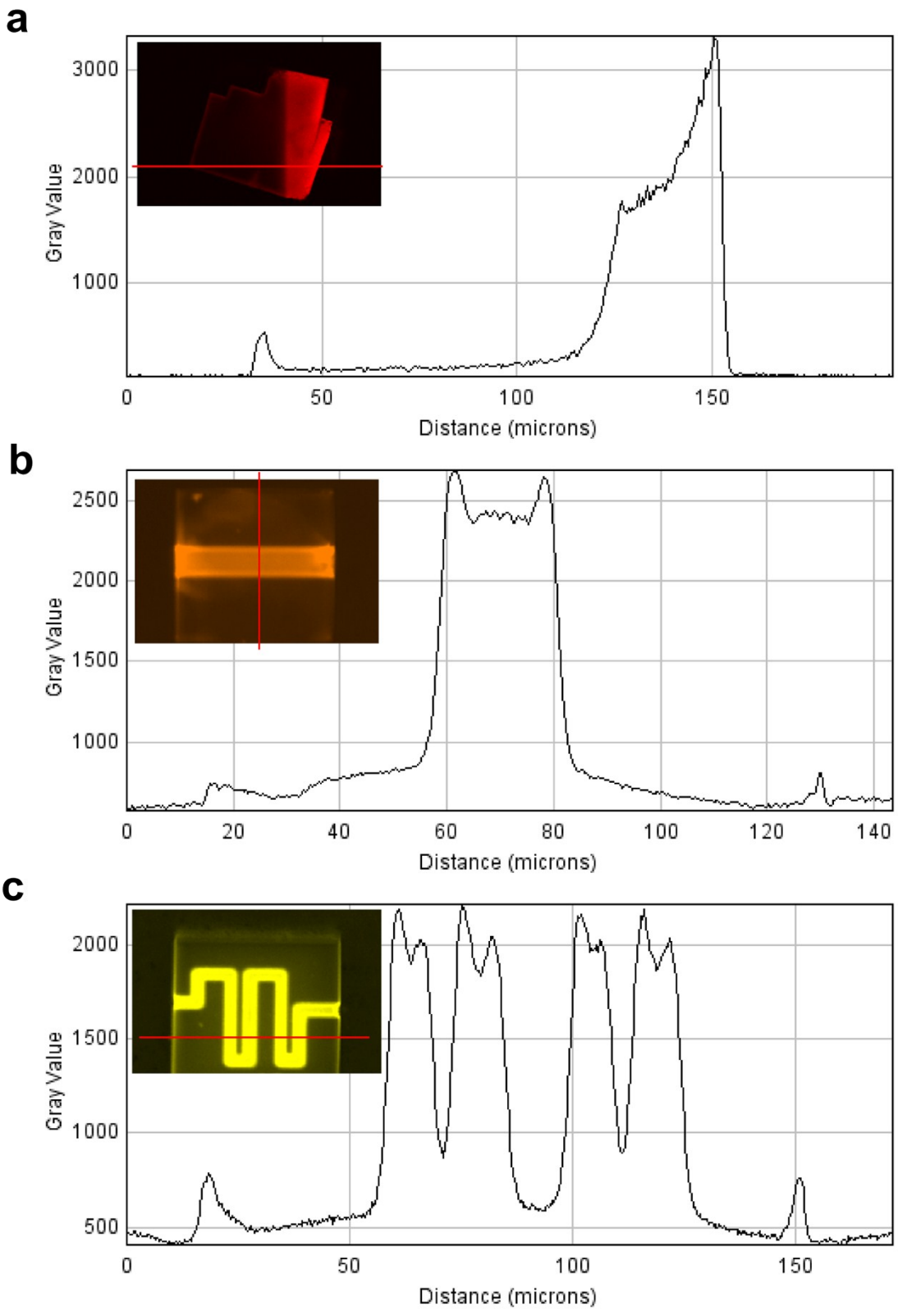

Figure S11. Grey value plot of selected line section for the images shown in Figure 2 of the article.

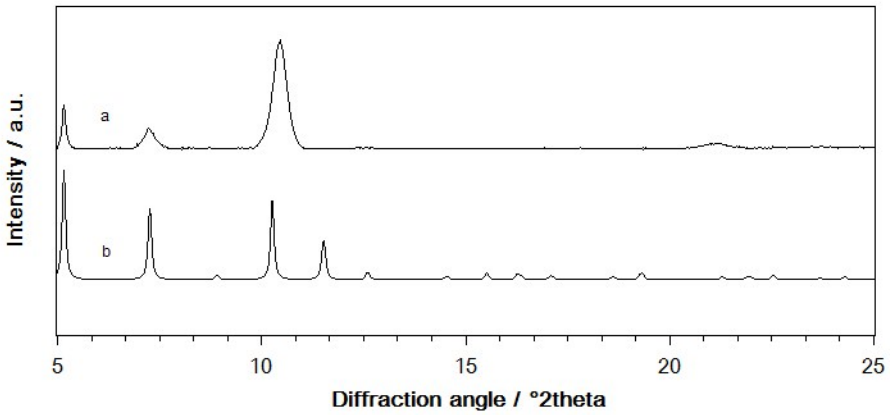

Figure S12. PXD pattern of a) IRMOF-10-$\mathbf{L_3}$ b) IRMOF-10 CSD Refcode XAMHEA.

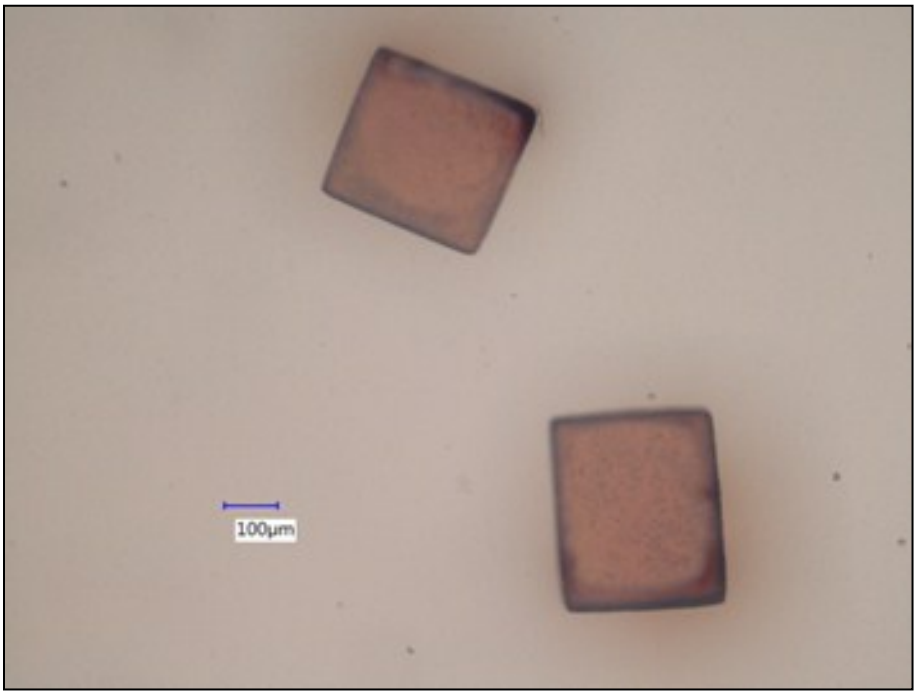

Figure S13. Light microscopy image of **IRMOF-10-$\mathbf{L_3}$** single crystals; dark orange. Scale bar: 100 µm.

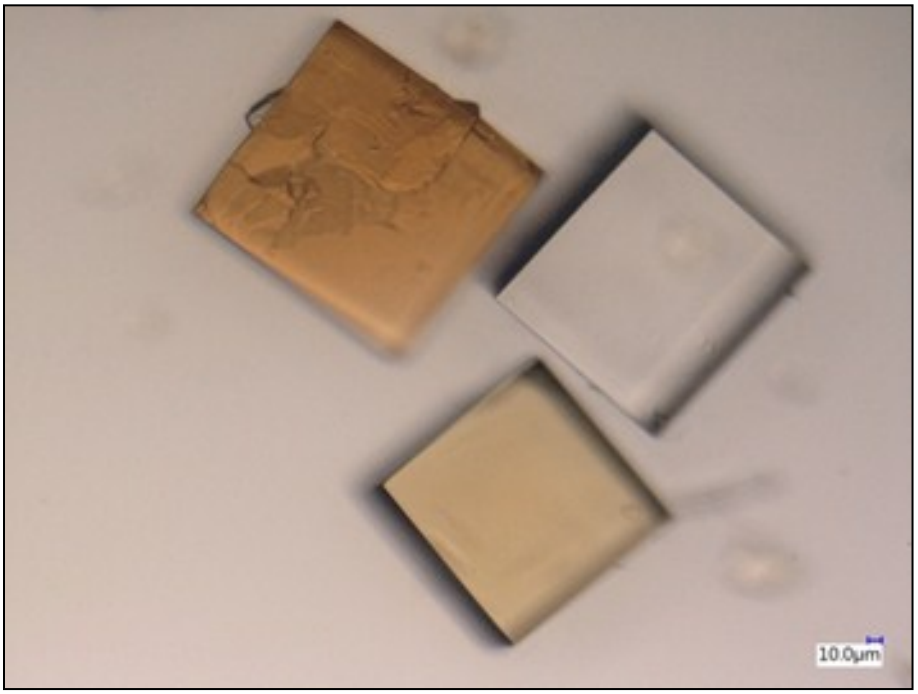

Figure S14. Light microscopy image for direct comparison of single crystal color: **IRMOF-1** (top right), **IRMOF-1-L_1/L_2** (bottom), **IRMOF-10-L_3** (top left). Scale bar: 10 µm.

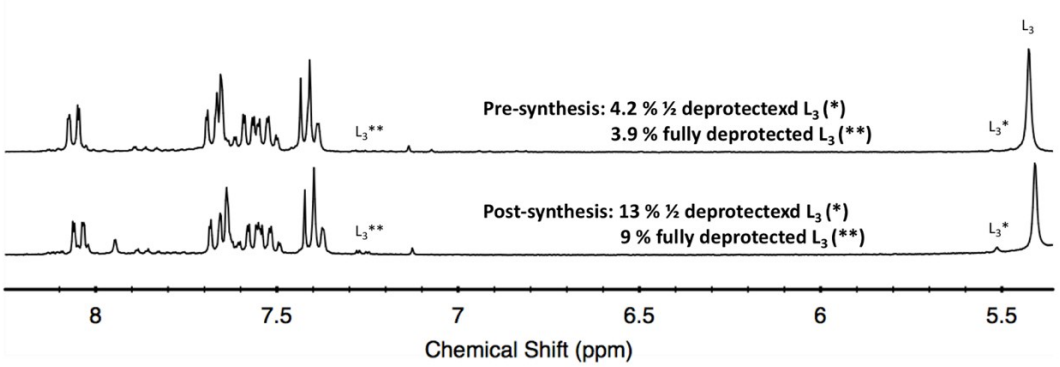

Figure S15. ^{1}H NMR spectra of a) linker **L_3** and b) IRMOF-10-**L_3** dissolved in a D2O/DMSO-d_6 solution. The percentage of post-synthesis deprotection was analyzed using the peaks described in Figure S3.

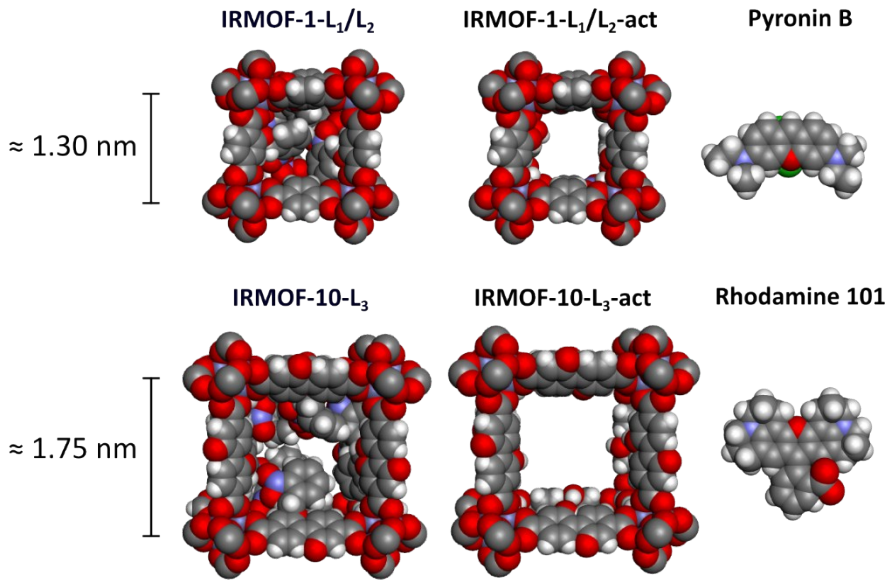

Figure S16. Space-filling structural representations of **IRMOF-1-L_1/L_2** and **IRMOF-10-L_3** and two representative dyes. The structures are based on literature and verified with X-ray diffraction (cell dimension of the cubic unit cell is indicated in the left). The *o*-nitrobenzyl pendant groups were added manually in arbitrary positions and the final structure was simulated using the force-field simulation option in the Discovery Studio software program (BIOVIA). Atom colors: red: O, dark grey: C, light grey: H, blue: N, green: Cl.

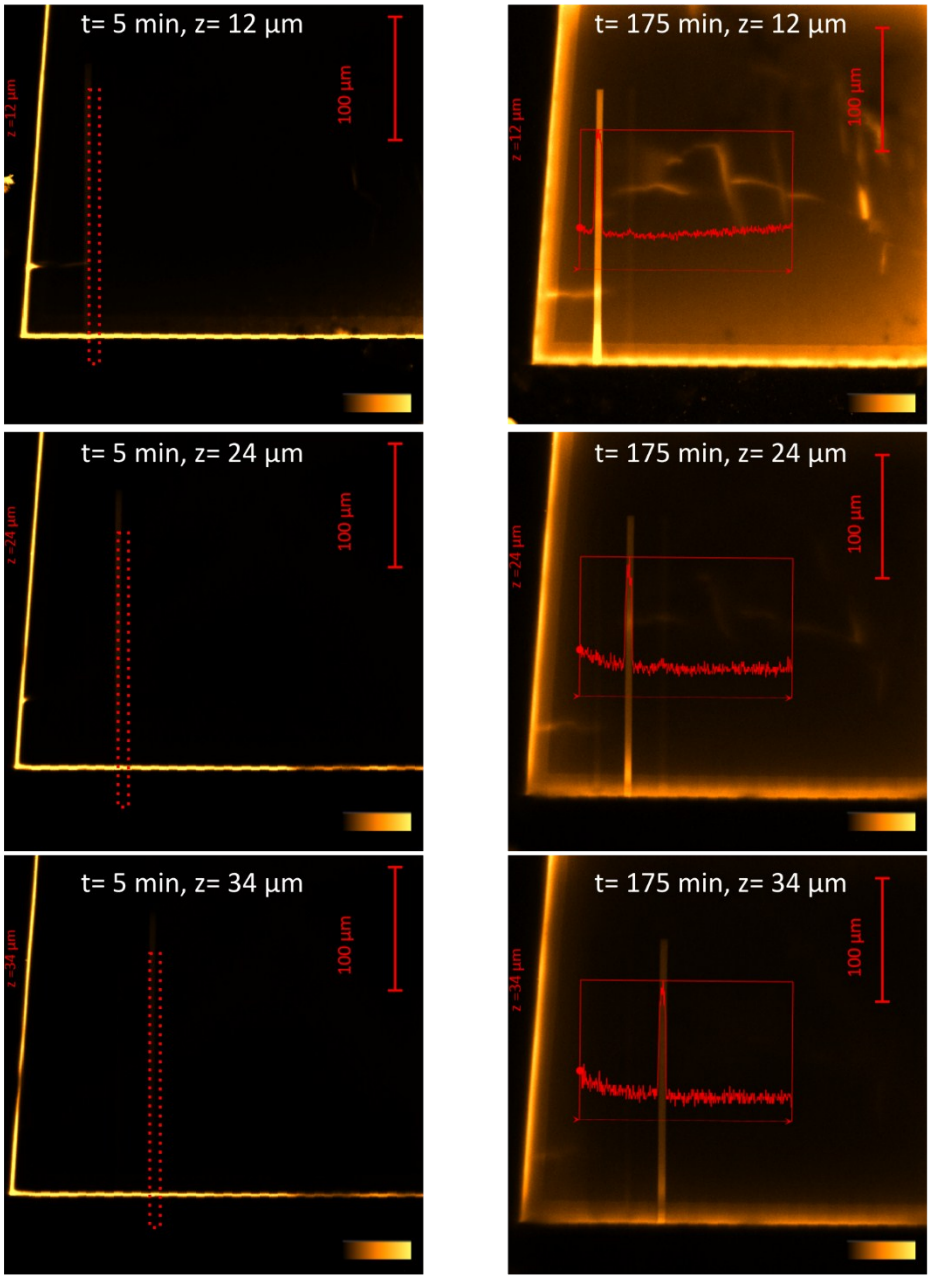

Figure S17. CLSM images of Rhodamine 101 (1 µM; λ_{em} = 600-700 nm; λ_{ex} = 561 nm) after direct laser writing of linear channels at different heights in an **IRMOF-10-L$_3$** crystal. Left: shortly after writing the channels (with 800 nm pulsed laser; indicated by the red-dotted area). Right: images at equivalent settings after 175 min; the insets are line profiles of the emission intensity. The relative intensity scale is shown in the right bottom of each image panel (0 - 256 a.u.). Scale bars 100 µm.

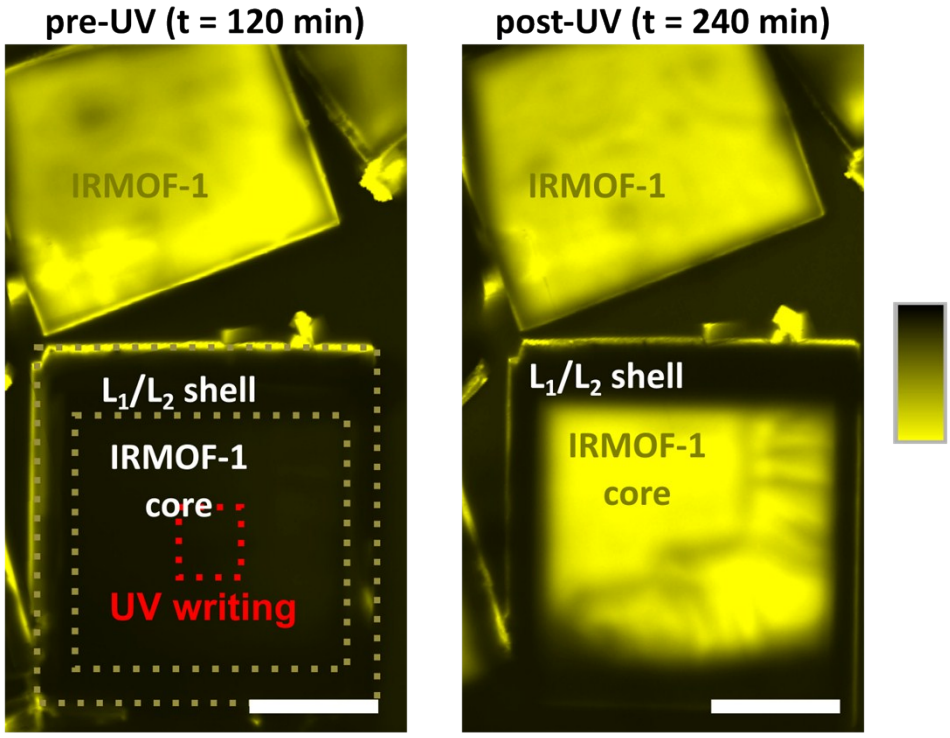

Figure S18. CLSM images of phototriggered dye uptake (Pyronin B; 1 µM; λ_{ex} = 559 nm) in **IRMOF-1-L_1/L_2@IRMOF-1** core-shell crystals. For reference, a IRMOF-1 crystal was added next to the core-shell heteroepitaxially assembled crystal. The image on the left shows the distribution of the dye after 120 min of soaking and before UV irradiation of the shell (indicated by the red-dotted area). Bright emission is only seen in the IRMOF-1 reference crystal and on the external surface of the core-shell assembly. The image on the right, by contrast to the initial situation, shows significant uptake of the dye in the IRMOF-1 core of the core-shell assembly at a next point in time 120 min after UV irradiation of the shell. The relative intensity scale of the images is shown in the right (0 - 4095 a.u.). Scale bars: 100 µm.

ESI-3. Synthesis procedures for the organic linkers

3.1. Synthesis of 2-((2-nitrobenzyl)oxy)terephthalic acid (L_1)

L_1 was synthesized following a sequence of two literature procedures (**Figure S19**). In a first step, 2-hydroxyterephtalic acid was synthesized from 2-aminoterepthalic acid using the method described by Hartmann *et al.*[4] Next, 2-((2-nitrobenzyl)oxy)terephthalic acid was synthesized from 2-hydroxyterephtalic acid using the procedure reported by Cohen *et al*.[5]

mp 280 °C; ^{1}H NMR (DMSO-d_6, 300 MHz): δ = 5.63 (s; 2H; CH_2), 7.64 ppm (m; 3H; ArH), 7.83 ppm (m; 2H; Ar'H), 8.09 ppm (d; J = 7; 1H; Ar'H), 8.19 ppm (dd; J = 8.2, 1.2; 1H; Ar'H), 13.27 ppm (s; 2H; COOH).

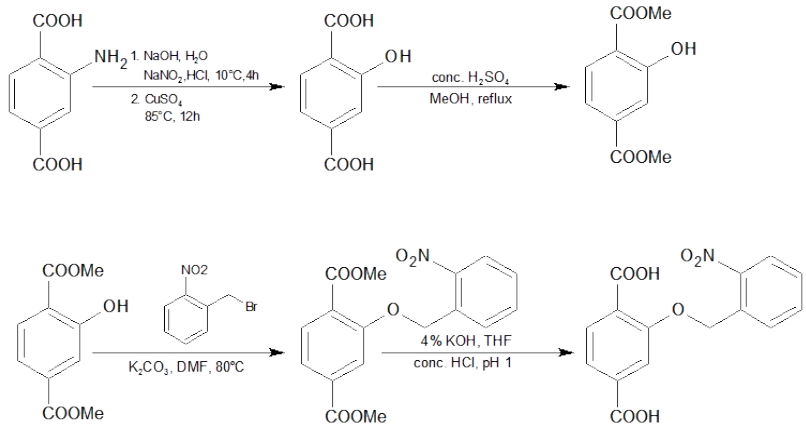

Figure S19. Synthesis route for 2-((2-nitrobenzyl)oxy)terephthalic acid (**L_1**)

3.2. Synthesis of 2,5-di((2-nitrobenzyl)oxy)terephthalic acid (L_2)

L_2 was synthesized following the scheme shown in **Figure S20**. The dimethyl ester of 2,5-dihydroxyterephtalic acid was synthesized following a procedure reported by Suzuki *et al*.[22] The next steps were performed as described below.

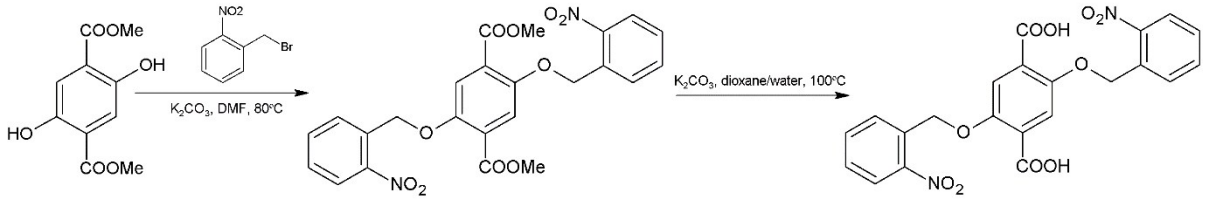

Figure S20. Synthesis route for 2,5-di((2-nitrobenzyl)oxy)terephthalic acid (**L_2**)

Synthesis of dimethyl 2,5-di((2-nitrobenzyl)oxy)terephthate (Me_2L_2)

2.72 g (12.0 mmol) of 2,5-dihydroxyterephtalic acid, 6.48 g (30.0 mmol) of 2-nitro(bromomethyl)benzene and 4.15 g (30.0 mmol) of K_2CO_3 in 100 ml of DMF were heated at 80°C under stirring for 2h. The initially yellow solution discolored within the first 30 min of

heating with formation of voluminous white precipitate. After cooling to room temperature, the slurry was poured in 200 mL of water and the well-separated precipitate was filtered off, washed by copious amount of water and 4 x 20 mL of THF to remove yellow-colored impurities. The yield of the snow-white **Me_2L_2** product was 5.67 g (95 %), after drying at 60 °C in air.

^{1}H NMR (DMSO-d_6, 300 MHz): δ = 8.16 (2H, d; J = 7.8; Ar'H), 7.99 (2H, d; J = 7.5; Ar'H), 7.86 (2H, t; J = 7.5; Ar'H), 7.65 (2H, d; J = 7.8; Ar'H), 7.56 (2H, s; ArH), 5.55 (4H, s; CH_2), 3.87 (6H, s; CH_3).

Synthesis of 2,5-di((2-nitrobenzyl)oxy)terephthalic acid (L_2)

In a one necked round-bottom flask equipped with a magnetic stirrer and a condenser, a solution of 6.08 g (44.0 mmol) of K_2CO_3 in 275 mL of deionized water was prepared. 275 mL of dioxane and 5.46 g (11.0 mmol) of **Me_2L_2** were added and the slurry was heated at a bath temperature of 100 °C under intensive stirring. The progress of the reaction was monitored by disappearance of the solid state. This occurred after approximately 5h10 min and the reaction was stopped after 5h40 min. The resulting transparent yellow solution was diluted by 1 L of deionized water and acidified by 20 mL of concentrated HCl after cooling down. The immediately formed yellow precipitate was filtered after 30 min and washed by copious amount of water. The yield of the crude product was 4.74 g in the form of a light yellow powder. Double recrystallization from dioxane and drying at 100 °C and 10 Torr yielded 3.15 g (61 %) of white **L_2** product with a light yellowish tint.

mp 273 °C; ^{1}H NMR (DMSO-d_6, 300 MHz): δ = 13.2 (2H, s; COOH), 8.17 (2H, d; J = 8.4; Ar'H), 8.04 (2H, d; J = 7.5; Ar'H), 7.83 (2H, t; J = 7.5; Ar'H), 7.63 (2H, d; J = 8.4; Ar'H), 7.51 (2H, s; ArH), 5.54 (4H, s; CH_2).^{13}C NMR (DMSO-d_6, 75 MHz): δ =166.3, 150.3, 146.8, 134.1, 132.8, 128.8, 128.8, 125.3, 124.7, 116.3, 67.6.

3.3 Synthesis of 2,2-Di((2-nitrobenzyl)oxy)biphenyl-4,4-dicarboxylic acid (L_3)

L_3 was synthesized following an eight step procedure (**Figure S21**). In the first steps, 3-hydroxybenzoic acid was used to produce 2,2'-dihydroxybiphenyl-4,4'-dicarboxylate (**VI**) through Ullmann coupling. These steps were based on the work by Sumby *et al.*[6], the modifications that were made are described below. The product was then functionalized to obtain **L_3** (**IX**).

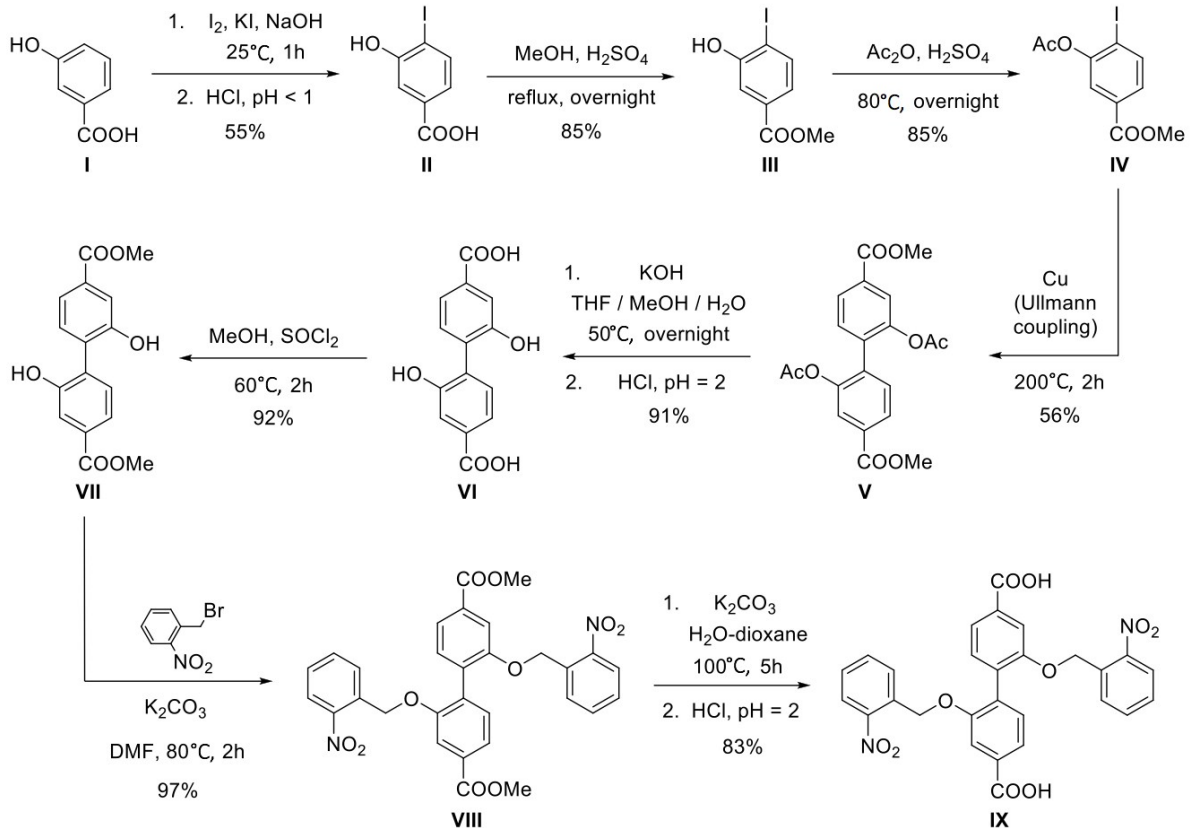

Figure S21. Synthesis route for 2,2-Di((2-nitrobenzyl)oxy)biphenyl-4,4-dicarboxylic acid (**L_3**)

Synthesis of 3-hydroxy-4-iodophenylcarboxylic acid (II)

Iodination of **I** was performed in alkaline aqueous medium. For this step, the procedure by Kolz *et al*. was followed,[7] no modifications were made but the yield obtained (55 %) was lower than previously described (64 %).

Synthesis of methyl 3-hydroxy-4-iodophenylcarboxylate (III)

II was esterified using methanol in an acid catalyzed reaction. The literature procedure was followed,[6] with adapted amounts for 18.5 g of starting material. The yield of the off-white solid after drying in air was 17.55 g (90 %).

^{1}H NMR (300 MHz, $CDCl_3$) δ = 7.76 (d, *J* = 8.2, 1H), 7.64 (d, *J* = 1.9, 1H), 7.33 (dd, *J* = 8.2, 1.9, 1H), 5.62 (s, 1H; OH), 3.91 (s, 3H; CH_3).

Synthesis of methyl 3-acetoxy-4-iodobenzoate (IV)

The only alteration that were made to the literature procedure was adapting the chemical amounts for 4 g of starting material **III**. The alcohol functional group on the aromatic ring of **III** is reacted with acetic anhydride to form an ester. The yield was 3.90 g (85 %) of white crystalline solid.

^{1}H NMR (300 MHz, $CDCl_3$) δ = 7.92 (d, *J* = 8.2, 1H), 7.73 (d, *J* = 1.9, 1H), 7.63 (dd, *J* = 8.2, 1.9, 1H), 3.91 (s, 3H; $ArOCOCH_3$), 2.39 (s, 3H; $ArCOOCH_3$).

Synthesis of dimethyl 2,2'-diacetoxybiphenyl-4,4'-dicarboxylate (V)

To perform the Ullmann coupling some minor modifications were made to the method described by Sumby *et al.* 8.0 g of **IV** was added to a Schlenk flask containing 8.0 g of activated copper powder and a Teflon-coated stirrer. The mixture was heated at 200 ˚C under N_2 for 1+1 h with a short interval in-between for mixing of the still hot reaction medium with a spatula, maintaining the protective atmosphere. After cooling down, the residue was treated by 4×30 mL of hot ethyl acetate and the extracts filtered through a silica plug. The filtrate was concentrated under reduced pressure and subjected to flash chromatography on silica using 2:5 ethyl acetate / hexane mixture (R_f = 0.61 and 0.33 for the starting compound and the product respectively). Yield of the almost white solid was 2.70 g (56 %).

^{1}H NMR (300 MHz, $CDCl_3$) δ = 7.99 (dd, *J* = 8.0, 1.5, 2H), 7.86 (d, *J* = 1.5, 2H), 7.39 (d, *J* = 8.0, 2H), 3.95 (s, 6H; ArOCOC**H$_3$**), 2.07 (s, 6H; ArCOOC**H$_3$**).

Synthesis of 2,2'-dihydroxybiphenyl-4,4'-dicarboxylic acid (VI)

For this step, no modifications were made to the literature procedure. The amounts were adapted for 2.70 g of **V** and 1.89 g (91 %) of the product in the form of a white solid was obtained.

mp 362 °C; ^{1}H NMR (300 MHz, DMSO-d_6) δ = 12.81 (s, 2H; ArCOOH), 9.74 (s, 2H; ArOH), 7.51 (s, 2H), 7.42 (d, *J* = 7.9, 2H), 7.27 (d, *J* = 7.9, 2H). ^{13}C NMR (101 MHz, DMSO-d_6) δ = 167.7, 155.1, 131.9, 131.4, 130.0, 120.1, 116.7.

Synthesis of dimethyl 2,2'-dihydroxybiphenyl 4,4'-dicarboxylate (VII)

In this step the carboxy groups of **VI** were protected by esterification. A two necked dry 100 mL round bottom flask equipped with a magnetic stirrer, a reflux condenser stoppered by a drying tube was charged with 50 mL of dry methanol. The flask was cooled down to 0 ˚C and 5 mL of thionyl chloride was added dropwise under stirring. 1646 mg of **VI** was added to the prepared solution at once and stirred until its complete dissolution. The mixture was heated up to 60 ˚C within 30 min and stirred at this temperature for 2 h. After cooling down the mixture to 30-40 ˚C, the solvent was removed by a nitrogen stream. The formed precipitate with some brownish residue was triturated with 10 mL of methanol, filtered out by suction filtration and washed by 3 × 30 mL of methanol. Yield of the white solid after drying in air was 1.67 g (92 %).

mp 291 °C; ^{1}H NMR (300 MHz, DMSO-d_6) δ = 9.84 (s, 2H; ArOH), 7.52 (d, *J* = 1.5, 2H), 7.44 (dd, *J* = 7.9, 1.5, 2H), 7.30 (d, *J* = 7.9, 2H), 3.85 (s, 6H; ArCOOC**H$_3$**). ^{13}C NMR (101 MHz, DMSO-d_6) δ = 166.6, 155.2, 132.0, 130.3, 130.2, 119.9, 116.5, 52.6.

Synthesis of dimethyl 2,2'-bis-((2-nitrobenzyl)oxy)-biphenyl-4,4'-dicarboxylate (VIII)

A 100 mL round bottom flask equipped with a magnetic stirrer bar was charged with 1510 mg of **VII**, 2592 mg of *o*-nitrobenzylbromide, 1658 mg of anhydrous potassium carbonate, and 50 mL of anhydrous DMF. The flask was closed and its contents was heated at 80 ˚C under stirring. After cooling down the content of the flask was emptied in 150 mL of water. The precipitate was separated by suction filtration, washed by 3 × 30 mL of water and 2 × 10 mL of hot methanol. The yield of the near-white solid after drying in air at 60 ˚C was 2.78 g (97 %).

mp 203 °C ^{1}H NMR (300 MHz, $CDCl_3$) δ = 8.06 (d, *J* = 6.4, 2H), 7.83 (d, *J* = 6.4, 2H), 7.72 (s, 2H), 7.44 – 7.34 (m, 8H), 5.36 (s, 4H; $ArCH_2Ar'$), 3.98 (s, 6H; $ArCOOCH_3$). ^{13}C NMR (75 MHz, $CDCl_3$) δ = 166.7, 155.5, 146.3, 134.0, 133.3, 132.3, 131.4, 128.3, 127.9, 124.9, 122.9, 113.0, 67.4, 52.4.

Synthesis of 2,2'-bis-((2-nitrobenzyl)oxy)-biphenyl-4,4'-dicarboxylic acid (IX)

286 mg of **VIII**, 300 mg of potassium carbonate in a mixture of 3 mL water and 3 mL of dioxane were placed in a screw cap vial equipped with a magnetic stirrer. The slurry in a sealed vial was heated at 100 ˚C for 5 h. The formed transparent yellow solution was cooled down, poured in 20 mL of water and acidified by concentrated aqueous hydrochloric acid to pH = 1-2. The immediately formed precipitate was separated by centrifugation, washed by 3 × 20 mL of water and 2 × 5 mL methanol, and dried at 60 ˚C in air until constant weight. The yield of the pale yellowish, almost white solid was 226 mg (83 %).

mp 312 °C; ^{1}H NMR (300 MHz, DMSO-d_6) δ = 13.17 (s, 2H; COOH), 8.06 (d, *J* = 6.6, 2H; ArH), 7.71 – 7.37 (m, 12H; Ar'H), 5.48 (s, 4H). ^{13}C NMR (101 MHz, DMSO-d_6) δ = 166.9, 155.1, 146.6, 133.8, 132.3, 131.8, 131.2, 131.2, 128.8, 128.2, 124.7, 122.1, 112.8, 66.8.

ESI-4. References

1 H. Deng, C. J. Doonan, H. Furukawa, R. B. Ferreira, J. Towne, C. B. Knobler, B. Wang and O. M. Yaghi, *Science*, 2010, **327**, 846–50.

2 K. Koh, A. G. Wong-Foy and A. J. Matzger, *Chem. Commun.*, 2009, 6162.

3 J. Schindelin, I. Arganda-Carreras, E. Frise, V. Kaynig, M. Longair, T. Pietzsch, S. Preibisch, C. Rueden, S. Saalfeld, B. Schmid, J.-Y. Tinevez, D. J. White, V. Hartenstein, K. Eliceiri, P. Tomancak and A. Cardona, *Nat. Methods*, 2012, **9**, 676–682.

4 D. Himsl, D. Wallacher and M. Hartmann, *Angew. Chem. Int. Ed.*, 2009, **48**, 4639–4642.

5 K. K. Tanabe, C. A. Allen and S. M. Cohen, *Angew. Chem. Int. Ed.*, 2010, **49**, 9730–9733.

6 D. Rankine, A. Avellaneda, M. R. Hill, C. J. Doonan and C. J. Sumby, *Chem. Commun.*, 2012, **48**, 10328.

7 A. Speicher, T. Backes, K. Hesidens and J. Kolz, *Beilstein J. Org. Chem.*, 2009, **5**, 71.